Available online at www.sciencedirect.com
ScienceDirect
Carbon 45 (2007) 2178–2187
CARBON
www.elsevier.com/locate/carbon

Shear properties of a carbon/carbon composite with non-woven felt and continuous fibre reinforcement layers

L.R. Bradley [a,*], C.R. Bowen [a], B. McEnaney [a], D.C. Johnson [b]

[a] *Materials Research Centre, Department of Mechanical Engineering, University of Bath, Bath BA2 7AY, United Kingdom*
[b] *Dunlop Aerospace Braking Systems, Holbrook Lane, Coventry CV6 4AA, United Kingdom*

Received 1 July 2006; accepted 25 June 2007
Available online 7 July 2007

Abstract

This study examines the shear properties of a 2D PAN-CVI carbon/carbon composite whose reinforcement layers are formed from a non-woven duplex cloth comprising a continuous fibre layer needled to a short fibre felt layer. Composites of three lay-ups were tested in several orientations using the Iosipescu (V-notched beam) shear test. Material anisotropy means that shear failure stresses and shear moduli are required in several orientations for structural analysis. It was necessary to mitigate the effect of specimen twisting by using strain gages on both sides of the specimens. The approximate ranges of measured shear failure stresses were 30–45 MPa in-plane and 8–22 MPa interlaminar. Shear moduli ranged between 6–16 GPa in-plane and 1–3 GPa interlaminar. While the presence of flaws in these composites leads to scatter in properties, the effect of bulk density on interlaminar properties was clearly observed.

1. Introduction

Carbon/carbon composites are now standard materials for aircraft disc brakes. Their widespread adoption is a result of a combination of properties suitable for this application [1,2], which include high heat capacity, good thermal conductivity, low coefficient of thermal expansion, adequate toughness and friction characteristics, retention of mechanical properties at elevated temperature and good strength to weight ratio. These characteristics result in significant weight savings, for example, 395 kg on a Boeing 767 [3] when compared to their sintered metal predecessors.

The subject of this study is a two-directional (2D) carbon/carbon composite whose reinforcement layers are formed from a non-woven duplex cloth composed of a continuous polyacrylonitrile (PAN) fibre layer attached to a short PAN fibre felt layer by needling. This duplex cloth can either be laid-up and jigged to form a 2D structure or laid-up and needled into a 3D preform. Similar reinforcement architectures are currently used in PAN-CVI carbon/carbon composites fabricated by a number of aircraft brake manufacturers, but the carbon/carbon composite studied here differs from these in having no needling through the thickness of the preform. This is because a greater degree of needling results in a larger number of fibres oriented perpendicular to the wear face; it has been shown that fibre orientations in which fibre ends emerge at the wear face are associated with higher wear rates due to their inhibition of friction film formation at low rotational speeds [4].

The principal objective of this study was to provide detailed and accurate measurements of in-plane and interlaminar shear properties of this technically important class of carbon/carbon composites that have the type of duplex carbon cloth reinforcement described above. Shear properties are important in the study of the operation of carbon/carbon composite aircraft brakes, for example, by structural finite element analyses. The study also provides an opportunity to evaluate the Iosipescu test methodology when applied to this type of carbon/carbon composite.

* Corresponding author. Fax: +44 1332 667118.
E-mail address: luke.bradley@rolls-royce.com (L.R. Bradley).

0008-6223/$ - see front matter © 2007 Elsevier Ltd. All rights reserved.
doi:10.1016/j.carbon.2007.06.072

2. Experimental

2.1. Materials

The carbon/carbon composite studied is composed of polyacrylonitrile derived carbon fibres in a pyrolytic carbon matrix. The basic structural element is a non-woven duplex cloth consisting of continuous filament tow needled to a cross-laid felt, which is subsequently carbonised. Within the duplex cloth, the preferred orientation of the fibres within the felt layer lay at 90° to the continuous fibre direction (Fig. 1a). The cloth was arranged into three different 2D lay-ups and placed between graphite jig plates while a carbon matrix of rough laminar morphology was deposited by chemical vapor infiltration. The composite was subsequently heat-treated to graphitise the matrix. The overall fibre volume fraction of the material is 20%, with approximately 75% of the fibres being in the continuous fibre layers.

Three different 2D lay-ups were used for assessment of shear properties. The duplex cloth layers were arranged such that the continuous fibres were aligned unidirectionally for the first lay-up and in a cross-ply arrangement for the second lay-up (Fig. 1b). These two lay-ups are, respectively, denoted zero–zero (ZZ) and zero–ninety (ZN) to avoid confusion with true unidirectional and cross-ply lay-ups, where felt layers are not present. The third lay-up was an approximately isotropic in-plane lay-up, in which the layers were arranged in zero–ninety (ZN) pairs with each pair rotated clockwise at 35° to the previous pair. Since this was not a true quasi-isotropic lay-up as conventionally defined [5], the term approximately isotropic (AI) is used in this paper.

2.2. Test specimens

Specimens were cut in the required orientation from a composite block of the appropriate lay-up, then milled and ground to the final dimensions specified by ASTM D 5379 [6], with a specimen thickness of 6 mm. This thickness corresponds to an even number of duplex layers (nominal thickness 1 mm), which was desirable so that specimens of the ZN lay-up contained equal numbers of zero and ninety degree layers. The necessity to machine specimens from a thicker piece of composite meant that it was not possible to ensure that the first layer was identical from specimen to specimen nor that there were full layers on each face. Furthermore, the nature of the AI lay-up combined with limitations on specimen thickness meant that the lay-up within the specimens could be neither balanced nor symmetric.

The 2D carbon/carbon composites used here can be approximated as orthotropic, but it is important to note that this is a greater approximation for the materials in this study than for composites reinforced with all continuous fibre due to the presence of both felt and continuous fibre layers. The number of distinct shear planes and their related Iosipescu shear specimen orientations are dependent upon the symmetry of the material.

Fig. 2 shows the six possible specimen orientations for an orthotropic layered composite. Material direction 1 is defined as parallel to the continuous fibres, material direction 2 as perpendicular to the continuous fibres but in the plane of the layers and material direction 3 as perpendicular to the plane of the layers, *i.e.*, the through-thickness direction. The composite with the ZZ lay-up approximates to orthotropic over a sufficient number of layers, with six distinct specimen orientations possible, while for the ZN and AI lay-ups there are fewer distinct orientations. Specimens were cut from material of all three lay-ups on the 1-2 and 1-3 shear planes to give in-plane and interlaminar shear properties, respectively. Specimens to test the ZZ lay-up on the 2-3 shear plane, for which this is a second interlaminar orientation, were also fabricated.

Walrath and Adams [7] do not recommend testing specimens in the 3-1 and 3-2 orientations since they are difficult to fabricate, easily damaged and give lower shear failure stresses than analogous test specimens in the 1-3 and 2-3 orientations even though the stress tensor is symmetrical. Additionally, since the stress states are nominally identical for such analogously oriented specimens (the stress tensor is symmetrical), the measured shear moduli should theoretically be the same. Thus, although tests in the 2-1, 3-1 and 3-2 shear planes appear to be unnecessary, a small number of tests were performed on these shear planes for the ZZ lay-up to check that the shear moduli were the same as those measured in the 1-2, 1-3 and 2-3 shear planes, respectively.

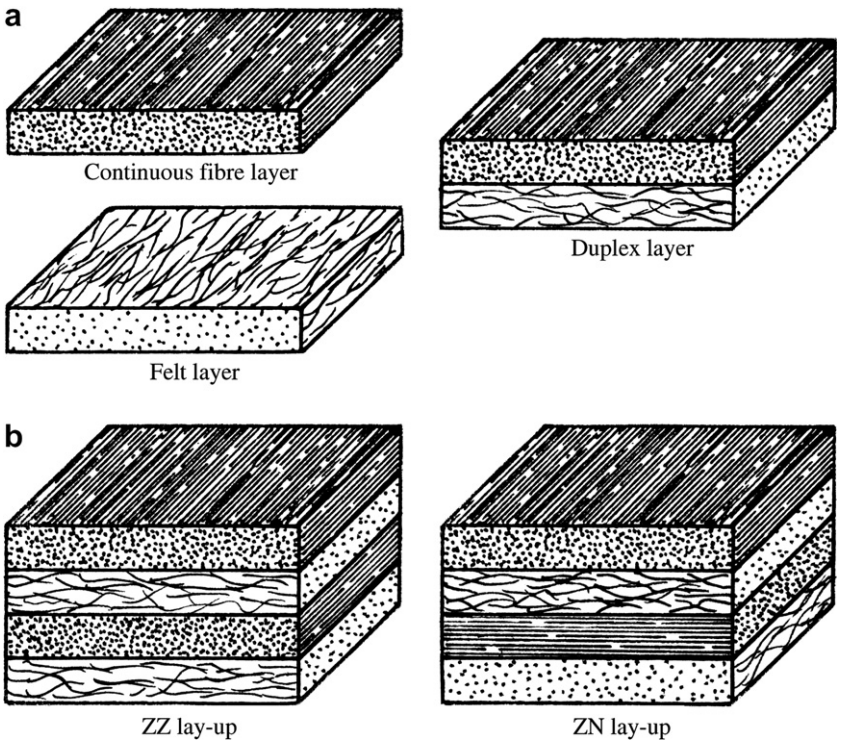

Fig. 1. (a) Illustration of layer types; (b) schematic of ZZ and ZN lay-ups.

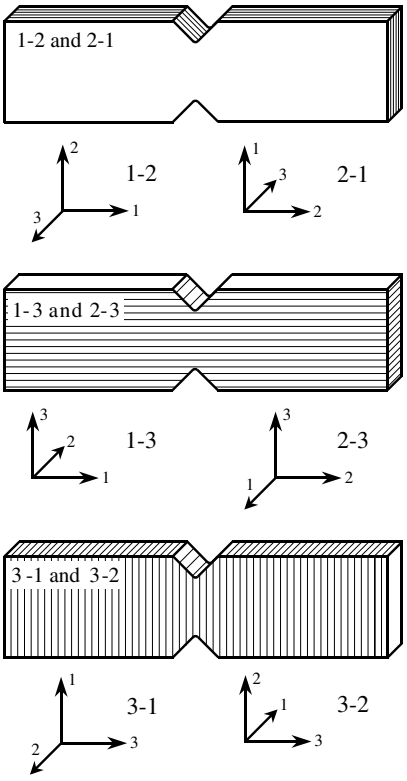

Fig. 2. Iosipescu specimen orientations.

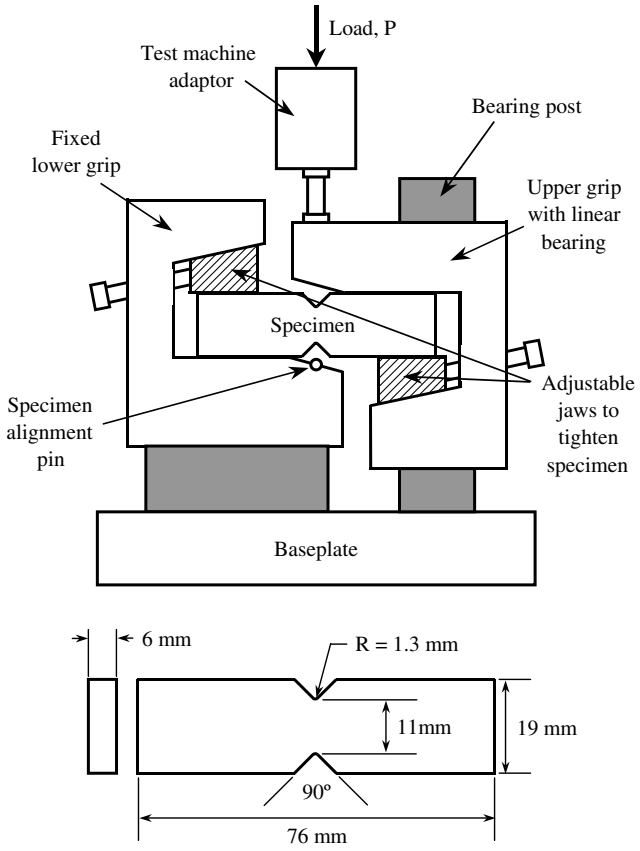

Fig. 3. Modified Wyoming test fixture; inset, specimen dimensions.

While processing conditions were carefully controlled to reduce pore blockage and preferential deposition of pyrolytic carbon close to the surface of the preform, some variation in porosity and therefore bulk density is unavoidable. It is important to account for variation in bulk density when comparing the effect on shear properties. Accordingly, the bulk density of each test specimen used in this study was measured by the Archimedes method, using deionised water as the immersion and infiltration liquid. The dry weight in air, W_a, was measured prior to vacuum infiltration, after which the water infiltrated weight underwater, W_b, and water infiltrated weight in air, W_c, were measured. The bulk density of each specimen, ρ_b, was calculated using Eq. (1), where ρ_l is the density of water at the temperature at which measurements were taken.

$$\rho_b = \rho_l \left(\frac{W_a}{W_c - W_b} \right) \tag{1}$$

Biaxial strain gages with ±45° grids (TML, FCT-2.350-11, grid length 2 mm) were attached to the specimens using cyanoacrylate adhesive (TML, Type CN). Solder tabs, required for the attachment of strain gage wires, were bonded to the specimens using silicone adhesive. The effect of out of plane torsion, termed 'specimen twisting', can introduce error in the shear modulus unless it is calculated using the average of strains measured on both faces of the specimen [8]. Furthermore, evaluation of initial specimens revealed specimen twisting greater than the 3% recommended by ASTM D 5379 as a threshold for the use of back-to-back strain gage readings. Therefore, strain gages were attached to both the front and back of all specimens.

2.3. Test method and procedure

Several test methods have been developed and extensively studied for the shear testing of composites [9,10]. Different test methods can give differing results for the same material; therefore many studies use multiple methods, *e.g.*, [11,12]. Broughton [10] recommended the plate twist and Iosipescu tests in his review on in-plane shear test methods. The method used in this study is the Iosipescu or V-notched beam shear test [6], which was selected for two main reasons. Firstly, it is the only composite shear test able to measure properties in all three material planes, enabling the measurement of both in-plane and interlaminar properties using the same method. Secondly, the test can measure both failure stresses and shear moduli, which many methods, for example the interlaminar short beam shear test [13], cannot. Furthermore, the short beam shear test gave unsatisfactory results when used to test the composite used in this study due to questionable failure modes.[1] Problems with the Iosipescu test methodology include stress concentrations at the specimen notches, which can affect the shear failure stress, plus a non-uniform stress distribution in the gage section and twisting of specimens, the last two of which can be remedied by correction factors and back-to-back strain gages, respectively. These are discussed further in Section 3.

The loading fixture used for the Iosipescu shear test (Fig. 3) is known as the 'modified Wyoming fixture' [14]. The fixture aims to produce a state of pure shear stress in the region between the notches by applying two counteracting force couples to the specimen, one either side of the notches, such that the induced moments cancel at the centre of the specimen. Tests were performed using a screw driven mechanical testing machine (Instron 1195) with a crosshead speed of 0.5 mm min^{-1}, a typical test being completed in approximately one minute. Loads and strains were recorded at a sampling rate of 4 Hz using a data-logging unit.

The average shear stress, τ, in the specimen gage section was obtained from the load, P, applied by the testing machine and the specimen cross-sectional area between the notches using Eq. (2), where w is the distance between the notches and t is the specimen thickness:

$$\tau = \frac{P}{wt} \tag{2}$$

[1] Bradley LR. Unpublished work, 2004.

The shear strain, γ, in the region between the two notches was calculated from the strains measured by the individual strain gage grids using Eq. (3), where ε_{+45° is the strain measured by the +45° grid and ε_{-45° the strain measured by the −45° grid. The shear strains measured on the front and back faces of each specimen were then averaged for use in the calculation of shear modulus:

$$\gamma = |\varepsilon_{+45^\circ}| + |\varepsilon_{-45^\circ}| \quad (3)$$

The shear modulus was calculated using a least squares linear fit to the portion of the stress–strain curve falling in the strain range 0.05–0.25%. This strain range is half the size of that recommended by ASTM D 5379 [6], with the lowest strain point lower than recommended, these changes being necessitated by the failure strain of the AI 1-2 specimens. Calculated over the same strain range, the shear modulus using the least squares method was found to differ from that using the shear chord method described in ASTM D 5379 by less than 1%. Specimen twisting was evaluated using Eq. (4), where G_a is the shear modulus measured on the front face of the specimen and G_b is the shear modulus measured on the back face of the specimen in the strain range used for modulus determination:

$$\text{Percent twisting} = |(G_a - G_b)/(G_a + G_b)| \times 100 \quad (4)$$

3. Results and discussion

3.1. Stress–strain response

The main feature of the stress–strain curves (Fig. 4) is their non-linearity, their gradually decreasing slope indicating a reduction in stiffness with increasing strain. The strain ranges in which the shear moduli were calculated, 0.05–0.25%, are indicated in Fig. 4. It is not known if the stress–strain curve is fully reversible from the higher end of the strains reached. Siron and Lamon [15] observed increasing hysteresis after loading and unloading to progressively higher loads a PAN-CVI carbon/carbon composite with bi-directional satin woven tow reinforcement needled in the through-thickness direction. Stress–strain responses of the Iosipescu shear specimens do not extend beyond failure since the strain gages were damaged or destroyed at this point. The behaviour of the specimens after the failure stress was reached can be seen in the plots of load versus test machine cross-head displacement (Fig. 5), which show that failure occurred 'gracefully' in most orientations, as is observed in many carbon/carbon composites.

3.2. Failure modes

The most common valid and invalid failure modes observed in Iosipescu shear testing of laminated composites are illustrated by Broughton [10] and in ASTM D 5379 [6]. An invalid failure mode occurs when a test specimen fails in a manner other than that intended, for example if failure initiates outside the specimen gage section or due to a stress other than that intended to cause failure. This results in the measured failure stress being lower than the true shear strength of the material. Invalid failure modes sometimes observed in the Iosipescu specimen include crushing at the loading points and crack initiation due to tensile stresses at the notch roots.

In-plane specimens of the ZN lay-up exhibited valid failure modes while many ZZ 1-2 specimens were affected by load point crushing. The interlaminar 1-3 specimens all exhibited valid failure modes of types illustrated in [6], for example the ZZ 1-3 specimens (Fig. 6a). In all ZZ 2-3

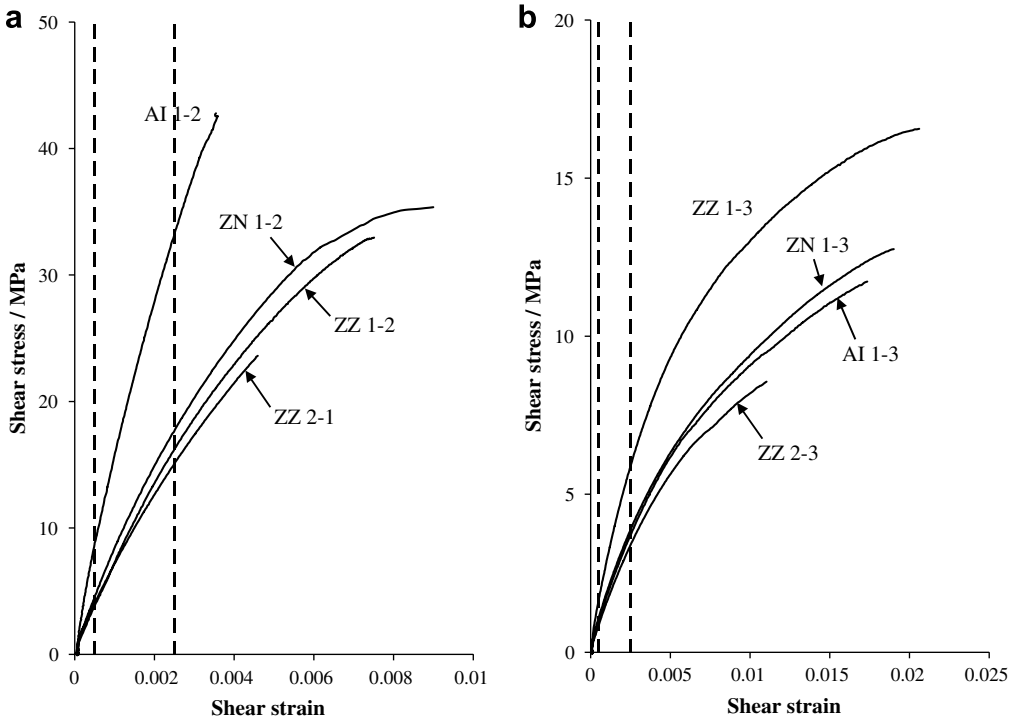

Fig. 4. Typical shear stress–strain plots (dashed lines bound the strain range used in the calculation of shear modulus). (a) In-plane; (b) interlaminar.

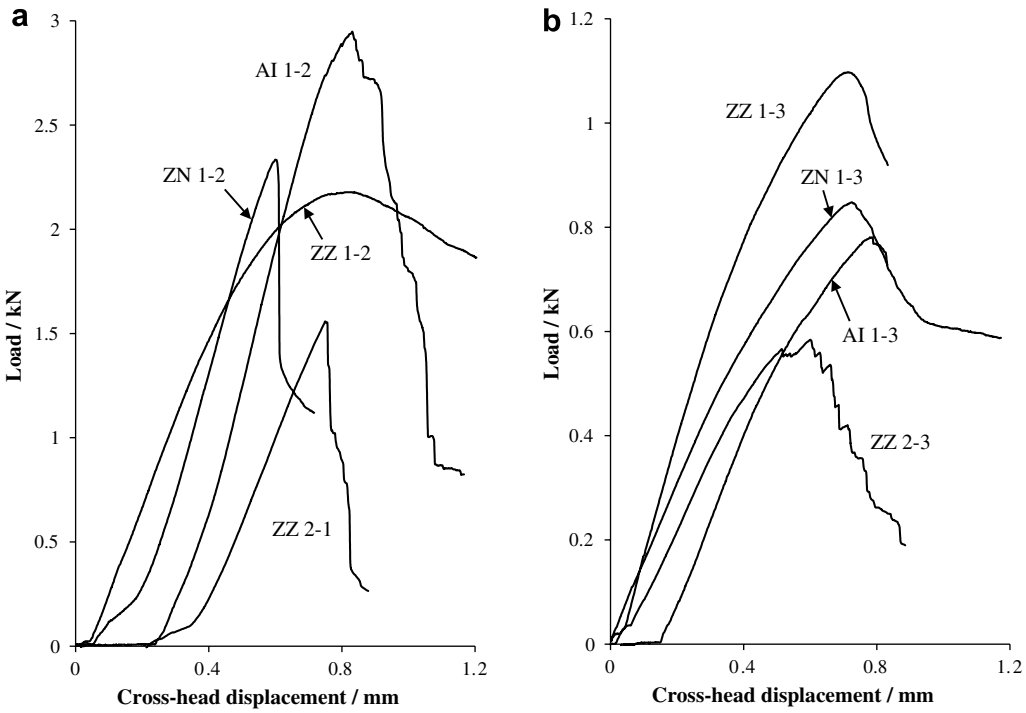

Fig. 5. Load versus test machine cross-head displacement. (a) In-plane; (b) interlaminar.

specimens cracks initiated at the notch radii and subsequently propagated into the specimen, Fig. 6b. As expected the ZZ 2-1, 3-1 and 3-2 specimens gave invalid modes. As there were sufficient valid failures to calculate an average failure stress for the ZZ 1-2 specimens, only the ZZ 2-3 specimen type was seriously affected by invalid failure modes. For all the AI 1-2 specimens the validity of failure was uncertain because of the distance over which cracks spread along the specimen.

3.3. Shear failure stresses

Table 1 shows average shear failure stresses for valid failures. Shear failure stresses are reported rather than shear strengths because the problems with the test method mentioned in Section 2.3 can potentially result in the measured failure stress being lower than the true shear strength. As expected, the average interlaminar shear failure stresses (10–16 MPa) are significantly lower than the in-plane values (34–41 MPa) due to lack of fibre reinforcement in the through-thickness direction.

For the in-plane tests, a trend of increasing shear failure stress with density is apparent for ZN 1-2 specimens, also for ZZ 1-2 specimens if valid and invalid failures are considered together (Fig. 7a). Examples of both valid and invalid failures exist at similar stresses and densities for the ZZ 1-2 specimen type, suggesting that failure of these specimens may be close to a boundary between valid and invalid modes. For the AI 1-2 specimens, it could not be determined whether there was a relationship between shear failure stress and bulk density, since the data were clustered into a narrow density range. Although most AI 1-2 specimens exhibited similar shear failure stresses to ZZ 1-2 and ZN 1-2 specimens of similar densities, some were higher. A higher failure stress was expected for the AI 1-2 specimens since fibres at angles other than 0° and 90° to the applied shear stress are subjected to tensile or compressive stresses, thereby increasing both the shear failure stress and stiffness of the composite by utilising the high axial strength and modulus of the fibres.

At the centre of the density range shown in Fig. 7b, the interlaminar shear failure stresses of the three lay-ups do not appear to differ greatly, excepting ZZ 2-3 specimens whose failure modes were invalid. This suggests that in-plane fibre arrangement does not have a prominent effect upon interlaminar failure stress. The wide density range of the ZZ 1-3 interlaminar specimens revealed a prominent correlation between shear failure stress and density. A similar increase in interlaminar shear failure stress with density has been observed in other carbon/carbon composites. For example, Casal et al. [16] measured the apparent interlaminar shear strengths of four different unidirectional PAN derived fibre-coal tar pitch matrix carbon/carbon composites at different porosities, finding them to rise by two to three times over the approximate bulk density range 1.5–1.7 g cm^{-3}.

3.4. Shear moduli

Table 2 shows that the average in-plane shear moduli are similar for the ZZ 1-2, ZZ 2-1 and ZN 1-2 specimen orientations. The slightly higher value for the ZN 1-2 specimens may be related to their slightly higher average density. The individual values of in-plane shear moduli

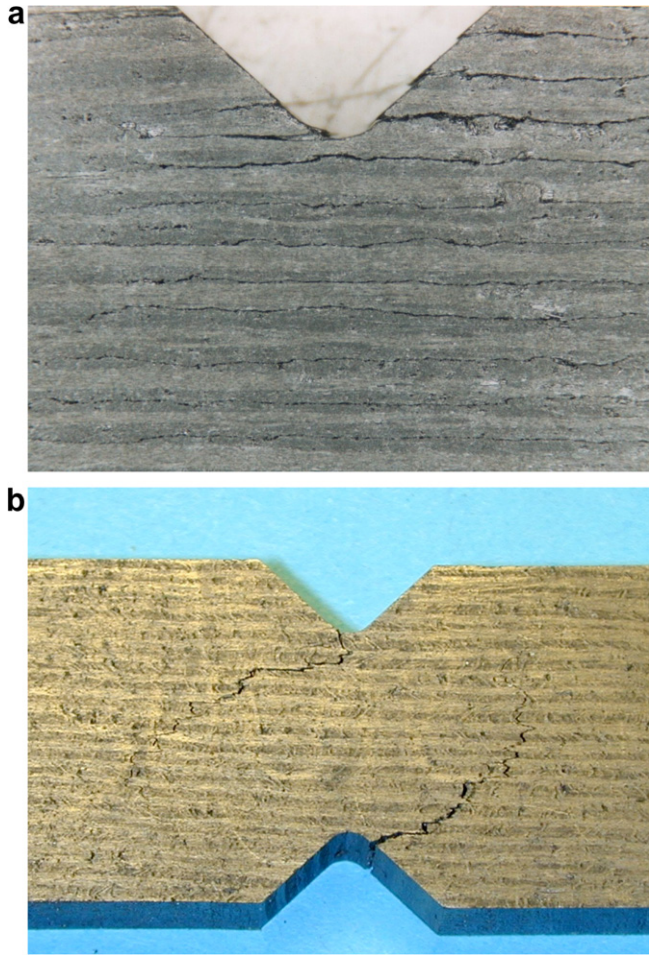

Fig. 6. Examples of failure modes observed during testing. (a) a ZZ 1-3, valid failure; (b) a ZZ 2-3, invalid failure.

Table 1
Average shear failure stresses and bulk densities for different lay-ups and shear planes (figures after ± signs represent one standard deviation)

Material lay-up	Shear plane	Bulk density (g cm^{-3})	Shear failure stress (MPa)	Sample size
In-plane				
AI	1-2[a]	1.84 ± 0.03	40 ± 4	10
ZN	1-2	1.81 ± 0.04	34 ± 2	10
ZZ	1-2[b]	1.92 ± 0.08	41 ± 4	5
Interlaminar				
AI	1-3	1.81 ± 0.03	12 ± 1	10
ZN	1-3	1.77 ± 0.03	10 ± 2	10
ZZ	1-3	1.89 ± 0.13	16 ± 3	12

[a] All 10 specimens exhibited failure modes whose validity was uncertain.
[b] Average failure stress calculated using valid failures only (hence reduced sample size).

for the ZN 1-2 and ZZ 1-2 orientations show a weak dependence on bulk density, Fig. 8a. The AI lay-up gave a much higher average shear modulus than the other lay-ups tested in-plane (Table 2). This is unsurprising since continuous fibre at angles other than 0° and 90° to the applied shear stress will be loaded in tension or compression, increasing in-plane shear stiffness. The shear moduli of the AI specimens are greatly scattered, Fig. 8a, probably because they could not be cut such that they contained identically oriented layers and especially since their thickness is much smaller than that over which the lay-up repeats.

Shear modulus correction factors can be applied to remove any error introduced by a non-uniform shear stress distribution across the gage section of the Iosipescu specimen, a phenomenon revealed by finite element studies, e.g., Pindera et al. [17]. For an orthotropic material, this distribution varies according to the orientation of the specimen with respect to the material directions. For a 0° in-plane (1-2) specimen, the shear stress at the strain gage is lower than the nominal shear stress hence the modulus may be overestimated, while for a 90° in-plane (2-1) specimen, the reverse is true. Ho et al. [18] showed the magnitude of these effects to be dependent upon the orthotropy ratio of the material:

$$\text{Correction factor} = 1.036 - 0.125 \times \log\left(\frac{E_1}{E_2}\right) \quad (5)$$

To investigate whether correction factors were necessary, the relationship between correction factor and orthotropy ratio given by Ho et al. (Eq. (5)) was used to estimate correction factors for the ZZ 1-2 and ZZ 2-1 specimens. The shear moduli measured on these two specimen orientations, in the absence of a non-uniform shear stress distribution across the gage section, should theoretically be identical due to the symmetry of the stress tensor. Since these specimens were very similar in average density (Table 2), any effect of density on shear modulus was unlikely to complicate this analysis. The orthotropy ratio was calculated from the averages of tensile and compressive Young's moduli [19] in material directions 1 and 2 (E_1 and E_2). Applying these factors changed the shear moduli for the ZZ 1-2 and ZZ 2-1 specimens from 6.2 and 5.8 GPa, respectively, to 5.8 and 6.6 GPa, respectively, i.e. it moved them past one other and further apart. Therefore, in this case application of these correction factors does not appear to confer a benefit. One possible reason for this might be that as noted by Broughton [10], ASTM D 5379 [6] specifies a notch root radius of 1.3 mm in order to promote a more uniform shear stress distribution along the notch root axis.

There is significant variation in average shear moduli between the interlaminar specimen types (Table 2). The average interlaminar shear modulus is highest for ZZ 1-3 specimens, but their higher average density than the specimens of other orientations, together with a prominent trend in density (Fig. 8b) makes direct comparison misleading. The interlaminar shear moduli of the ZZ 3-1 and 3-2 specimens are lowest, but their average densities are also lower (Table 2) and their shear moduli are similar to 1-3 and 2-3 specimens of equivalent densities (Fig. 8b).

The shear moduli of ZZ 3-1 and 3-2 specimens should theoretically be the same as ZZ 1-3 and 2-3 specimens, respectively, which if density is taken into account appears

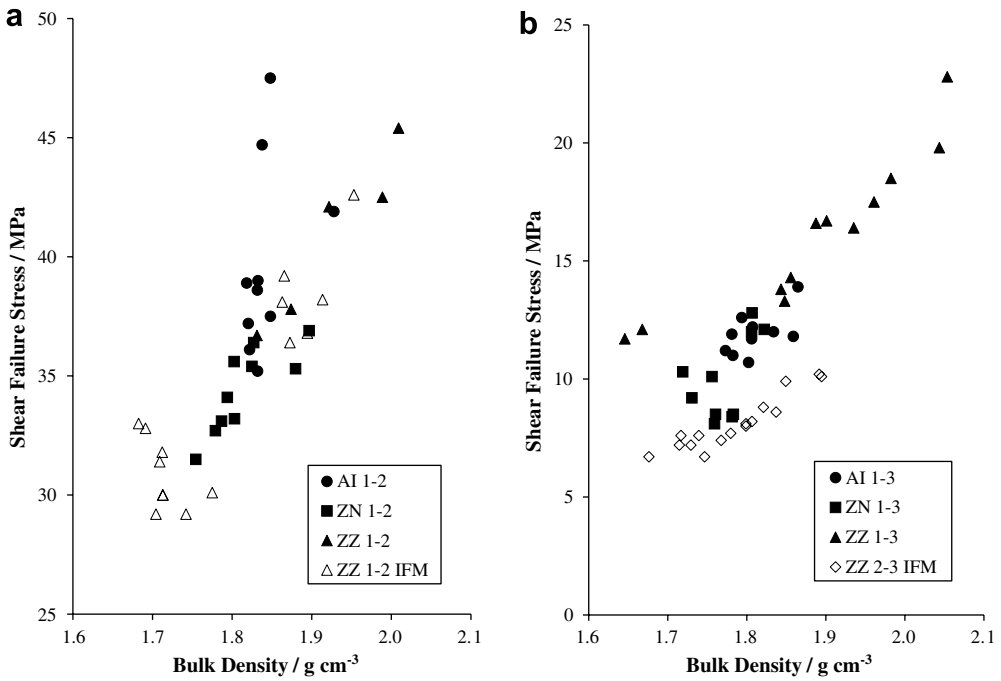

Fig. 7. Shear failure stresses for individual specimens plotted versus bulk density (IFM = invalid failure mode). (a) In-plane; (b) interlaminar.

Table 2
Average shear moduli, bulk densities and specimen twisting for different lay-ups and shear planes (figures after ± signs represent one standard deviation)

Material lay-up	Shear plane	Bulk density (g cm^{-3})	Shear modulus (GPa)	Average specimen twisting (%)	Sample size
In-plane					
AI	1-2	1.84 ± 0.03	12 ± 2	15	10
ZN	1-2	1.81 ± 0.04	6.4 ± 0.4	24	10
ZZ	1-2	1.73 ± 0.05	6.2 ± 0.4	14	10
ZZ	2-1	1.72 ± 0.01	5.8 ± 0.6	36	5
Interlaminar					
AI	1-3	1.81 ± 0.03	1.3 ± 0.1	5	10
ZN	1-3	1.78 ± 0.04	1.4 ± 0.2	7	5
ZZ	1-3	1.89 ± 0.13	2.1 ± 0.6	7	12
ZZ	2-3	1.77 ± 0.06	1.1 ± 0.1	4	12
ZZ	3-1	1.68 ± 0.05	1.2 ± 0.1	45	5
ZZ	3-2	1.70 ± 0.04	0.9 ± 0.1	28	5

approximately so (Fig. 8b). For some of the interlaminar specimen orientations, the density range of the specimens is too small for a relationship between shear modulus and density to be ascertained. Nevertheless, the prominent trend apparent for the ZZ 1-3 specimens suggests that the effect of density on shear modulus is significant and of similar magnitude to the relationship between density and shear failure stress.

To better compare the interlaminar shear moduli of the three lay-ups; estimates were made of these at 1.85 g cm^{-3}, which is the typical bulk density of the composite. With the effect of density removed, the shear moduli are in the following descending order: ZZ 1-3, ZN 1-3, AI 1-3 and ZZ 2-3 (Table 3). This is the same order observed by Zhou et al. [20] for a carbon–epoxy composite, where the interlaminar (1-3) shear moduli were found to decrease steadily from unidirectional to cross-ply to quasi-isotropic lay-ups, with the unidirectional 2-3 shear modulus lower still. This order was attributed to the corresponding reduction in the number of fibres along the length of the specimen.

3.5. Specimen twisting

The presence of strain gages on both faces of each specimen allowed the estimation of twisting for each specimen. Of interest is the general magnitude of specimen twisting and whether this was related to the lay-up and orientation used. Average specimen twisting for the different lay-ups and specimen orientations calculated using Eq. (4) can be grouped according to the magnitude of twisting, Table 2. In-plane specimens (excluding the 2-1 orientation) exhibited appreciable average specimen twisting (14–24%). Interlaminar specimens (excluding the 3-1 and 3-2 orientations) exhibited the lowest average twisting (4–7%). Specimens of the 2-1, 3-1 and 3-2 orientations exhibited high average twisting (28–45%). In other studies Morton et al. [8] observed that specimen twisting was significant and therefore the use of back-to back gages was important for 90° unidirectional (2-1) and 0/90° cross-ply (1-2), but not 0° unidirectional (1-2) graphite–epoxy in-plane specimens. Pierron and Vautrin [12] found that strain averaging between the two faces eliminated a significant amount of scatter in a study involving in-plane specimens. Gipple and Hoyns [21] thoroughly investigated the interlaminar shear response of thick section composite materials by the Iosipescu method and found strain differences between

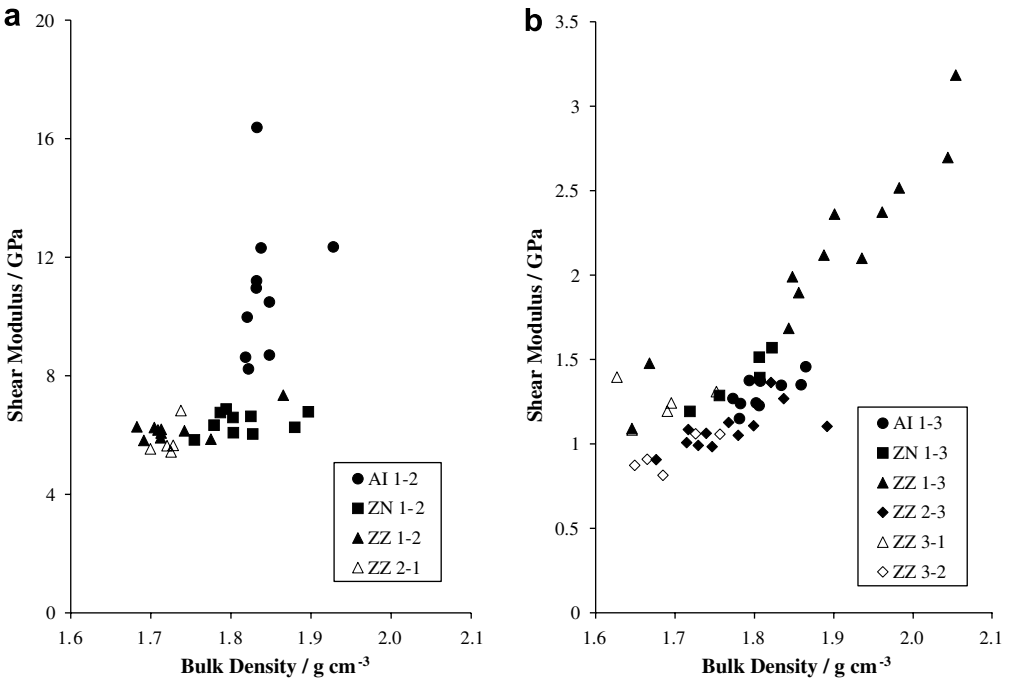

Fig. 8. Shear moduli plotted versus bulk density. (a) In-plane; (b) interlaminar.

Table 3
Estimated interlaminar shear moduli at a bulk density of 1.85 g cm^{-3}

Material lay-up	Shear plane[a]	Shear modulus (GPa)
ZZ	1-3	2.0
ZN	1-3	1.6
AI	1-3	1.4
ZZ	2-3	1.2

[a] The remaining orientations have too few data points for the method used to estimate properties at a density of 1.85 g cm^{-3} to be meaningful.

the front and back of the specimens to be insignificant. Together, these studies suggest specimen twisting is worse for in-plane than interlaminar specimens, as was observed in the current work (excluding the 3-1 and 3-2 orientations).

Some twisting is known to arise from the design of the modified Wyoming fixture, which does not provide sufficient lateral constraint to the specimens to prevent displacement of the movable half of the fixture outside the plane of loading [10]. The orientation of continuous fibres with respect to the loading surfaces of the specimens can also influence twisting; Morton et al. [8] suggested that 90° unidirectional and 0/90° cross-ply specimens were more susceptible to twisting than 0° unidirectional ones because the local hardness of the fibres emerging at 90° to the loading surface was high, thus reducing deformation of local asperities that would otherwise distribute the load more evenly across the thickness. This may explain the high specimen twisting observed in the 2-1 and 3-1 orientation specimens, in which continuous fibre emerges perpendicular to the loading surface. The high specimen twisting in the 2-1, 3-1 and 3-2 orientation specimens may also be explained by the fact that they possess little or no fibre reinforcement along their length; consequently, their torsional rigidity is lower than that of specimens with continuous fibres along their length, making them less able to withstand twisting. This may explain why the 3-2 specimens, which have no continuous fibre emerging perpendicular to the loading face, still exhibited significant twisting, although not as much as the 2-1 and 3-1 specimens. Furthermore, a similar carbon/carbon composite comprised of felt layers only, with the preferred fibre orientations within all layers aligned parallel to each other and orientated along the length of the specimen, *i.e.*, with none perpendicular to the loading surfaces, exhibited an average specimen twisting of 28%.[2] A further probable cause of twisting for the in-plane specimens is the asymmetric nature of the lay-ups within the specimens, which can result in out-of-plane twisting when loaded. The difference in average specimen twisting between the in-plane and interlaminar specimens (excluding the 2-1, 3-1 and 3-2 orientations) may be partially explained by this. The AI and ZN lay-ups are clearly not symmetric, while the presence of the felt layers means that unlike a true unidirectional composite, even the ZZ lay-up is not symmetric.

Twisting may affect the failure stress of the specimens. Morton et al. [8] state that it is probable that the apparent shear strength (*i.e.* shear failure stress) will increase as twisting is reduced or eliminated. For the interlaminar specimen orientations where twisting was low, it seems unlikely that the measured shear failure stresses were greatly affected, while for the in-plane specimens with intermediate average specimen twisting, the reduction in shear

[2] Bradley LR. Unpublished work, 2002.

failure stresses may be significant. For the specimen orientations that exhibited excessively high twist (ZZ 2-1, ZZ 3-1 and ZZ 3-2), the shear failure stresses are not reported in Table 1 owing to invalid failure modes. However, a quantitative estimate of the effect of twisting upon the shear failure stress is beyond the scope of the current study. It appears that there has been little discussion in the literature of this effect for carbon–epoxy composites and none for carbon–carbon composites; therefore, this is a possible area for future work.

3.6. General discussion

In-plane failure stresses are in a similar range (27–35 MPa) to those measured using the Iosipescu method by Neumeister et al. [22], on a composite comprised of T-300 carbon fibres and a pyrolysed K-650 phenolic matrix in a variety of 1D and 2D lay-ups. This excludes a quasi-isotropic lay-up whose in-plane shear failure stress was higher than that of the AI lay-up of the current study, probably due to a higher volume fraction of continuous fibres. The in-plane shear moduli of the ZZ and ZN lay-ups, around 6 GPa, are comparable to literature values of the in-plane shear moduli of 2D carbon/carbon composites. For example, Neumeister et al. [22] measured initial in-plane shear moduli of 5.0–6.5 GPa (excluding quasi-isotropic), with a value of 6.0 GPa for a cross-ply lay-up. Siron and Lamon [15] reported an initial in-plane modulus of 5.8 ± 0.2 GPa for a PAN-CVI carbon/carbon composite with bi-directional satin woven tow reinforcement needled in the through-thickness direction. The in-plane shear moduli, of the ZZ and ZN lay-ups are slightly higher than those reported for unidirectional and cross-ply carbon–epoxy laminates, which are in the region of 4–5 GPa [10,20,23], and the shear modulus of single crystal graphite, 4.5 GPa [24]. Although the felt layers might be expected to reduce the in-plane shear modulus compared to a case where all layers contain continuous fibre, this is not so, probably because the in-plane shear modulus of the felt layers is higher than expected. This was measured using a similar carbon/carbon composite reinforced with felt layers only, with the preferred fibre orientations of all layers aligned parallel to the long axis of the specimen [19]. The mean modulus was 5.3 GPa, measured on four Iosipescu specimens of average bulk density 1.83 g cm^{-3}.

Typical interlaminar failure stresses of 12–13 MPa at the centre of the specimen density range compare well with the figures given for 1D and 2D carbon/carbon composites (10.5–12.4 MPa) by Neumeister et al. [22]. For the AI lay-up interlaminar failure stresses are close to those measured on the same composite by the double punch shear test method [25], *i.e.* 10 MPa with a standard deviation of 2 MPa,[3] measured using 100 specimens of average bulk density 1.87 g cm^{-3}. The interlaminar shear moduli measured for all lay-ups tested, 1–3 GPa, are in the same region as those measured using a resonant beam method ($G_{13} = 1.9$ GPa) by Domanovich et al. [26] for a 2D PAN fibre phenolic resin matrix carbon/carbon composite of bulk density 1.62 g cm^{-3}, heat treated at 2400 °C. That the interlaminar modulus is so much lower than the in-plane modulus of the felt layers suggests the preferred orientation of the short fibres in the felt layers has a significant effect upon modulus.

It seems likely that given the amount of specimen twisting measured, future tests involving similar carbon/carbon composites would benefit from the use of an Iosipescu fixture redesigned to reduce twisting, such as that used by Pierron and Vautrin [12]. This is desirable because although the modulus is unaffected when back-to-back strain measurement is used, the effect of twisting upon the failure stresses is uncertain. Thicker specimens also seem advisable given the thickness of the duplex layers, although whether their use would reduce the scatter observed in the properties of this composite is debatable. The scatter in interlaminar failure stress (1 s.d. = 20%) measured by the double punch shear method, for which the sample size of 100 was much larger than that of the Iosipescu tests, is no smaller than that generally observed in the interlaminar Iosipescu results over a similar density range (Table 2). This suggests this level of scatter may be inherent to the material, reflecting, for example, the variation in void content. Similar scatter is also apparent in the compressive and tensile properties of this material [19].

4. Conclusions

The shear properties of 2D PAN-CVI carbon/carbon composites with alternating felt and continuous fibre layers were evaluated in several orientations using the Iosipescu test. Three composite lay-ups were tested, namely zero–zero, zero–ninety and an approximately quasi-isotropic lay-up. In-plane failure stresses varied between approximately 30 and 45 MPa while interlaminar failure stresses ranged from approximately 8 to 22 MPa, with 12–13 MPa typical at the centre of the specimen density range. Significant increases in both in-plane and especially interlaminar failure stresses with increasing bulk density were observed for specimen types with a sufficiently wide density range. Density appeared to have a greater effect than lay-up upon interlaminar shear failure stresses. The shear stress–strain response of the material was non-linear with no abrupt change in slope apparent. This was most pronounced for interlaminar specimens and was least so for the approximately isotropic lay-up tested in-plane. Although most specimens exhibited valid failure modes, some invalid and some inconclusive failure modes occurred for certain combinations of lay-up and orientation.

The in-plane shear moduli of the zero–zero and zero–ninety lay-ups were similar to one another (~6 GPa) and slightly higher than for a typical unidirectional carbon–epoxy. They appeared weakly related to bulk density.

[3] Bradley LR. Unpublished work, 2004.

The in-plane shear modulus of the approximately isotropic lay-up was higher and scattered (8–16 GPa). Interlaminar shear moduli varied from approximately 1 to 3 GPa. A prominent relationship with bulk density was revealed when individual specimens of the same type were spread over a wide enough density range.

Two issues were considered regarding the performance of the Iosipescu test: specimen twisting and the need for correction factors. Specimen twisting evidenced by back-to-back strain gage measurements was smaller for interlaminar than for in-plane specimens, excluding the 2-1, 3-1 and 3-2 orientations, which exhibited significant twisting. Shear moduli were unaffected by specimen twisting due to the use of back-to-back strain gages. To reduce this twisting, a redesigned Iosipescu fixture is recommended for future tests, together with thicker specimens. The specimen twisting observed is likely to result in the reported shear failure stresses being conservative estimates of the shear strength; an investigation to quantify this effect would be interesting future work. An analysis of the ZZ 1-2 and ZZ 2-1 shear moduli suggested that application of correction factors did not appear to confer a benefit in this study. The scatter observed in all of the properties measured is more likely to be an inherent property of the material rather than an artefact of the test method.

As noted in Section 1, similar PAN-CVI carbon/carbon composites comprising duplex felt-continuous fibre layers, but with through-thickness needling, are used in aircraft brake discs by a number of manufacturers. Since the composite studied was only needled within layers, further work looking at 3D needled composites would be useful. The addition of through-thickness needling is expected to increase the interlaminar shear properties compared to those measured in this study. The shear properties of the composites used in this work should be used with caution in finite element analysis of brake discs because the general scatter in the properties is large and the sample sizes are smaller than is ideal for the calculation of design basis values. Furthermore, the shear modulus reduces with increasing applied stress, especially in the interlaminar orientations, indicating that non-linear elastic elements may be desirable for finite element analysis.

Acknowledgements

The authors would like to thank the Engineering and Physical Sciences Research Council and Dunlop Aerospace for their financial support and Dunlop Aerospace for providing the carbon/carbon composites studied.

References

[1] Ruppe J. Today and the future in aircraft wheel and brake development. Can Aeronaut Space J 1980;26(3):209–16.
[2] Stimpson IL, Fisher R. Design and engineering of carbon brakes. Philos Trans R Soc Lond A 1980;294:175–82.
[3] Awasthi S, Wood JL. C/C composite materials for aircraft brakes. Adv Ceram Mater 1988;3(5):449–551.
[4] Hutton TJ, Johnson D, McEnaney B. Effects of fibre orientation on the tribology of a model carbon–carbon composite. Wear 2001;249(8):647–55.
[5] ASTM Designation: D 3878. Standard terminology for composite materials; 2000.
[6] ASTM Designation: D 5379/D 5379M. Standard test method for shear properties of composite materials by the V-notched beam method; 1998.
[7] Walrath DE, Adams DF. The Iosipescu shear test as applied to composite materials. Exp Mech 1983;23:105–10.
[8] Morton J, Ho H, Tsai MY, Farley GL. An evaluation of the Iosipescu specimen for composite materials shear property measurement. J Compos Mater 1992;26(5):708–50.
[9] Adams DF, Lewis EQ. Current status of composite material shear test methods. SAMPE J 1994;31(6):32–41.
[10] Broughton WR. Shear. In: Hodgkinson J, editor. Mechanical testing of advanced fibre composites. Cambridge: Woodhead Publishing; 2000. p. 100–23 [Chapter 6].
[11] Lee S, Munro M, Scott RF. Evaluation of three in-plane shear test methods for advanced composite materials. Composites 1990;21(6):495–502.
[12] Pierron F, Vautrin A. Accurate comparative determination of the in-plane shear modulus of T300/914 by the Iosipescu and 45° off-axis tests. Compos Sci Technol 1994;52(1):61–72.
[13] ASTM Designation: D 2344/D 2344M. Standard test method for short-beam strength of polymer matrix composite materials and their laminates; 2000.
[14] Adams DF, Walrath DE. Further development of the Iosipescu shear test method. Exp Mech 1987;27(2):113–9.
[15] Siron O, Lamon J. Damage and failure mechanisms of a three-directional carbon/carbon composite under uniaxial tensile and shear loads. Acta Mater 1998;46(18):6631–43.
[16] Casal E, Granda M, Bermejo J, Bonhomme J, Menéndez R. Influence of porosity on the apparent interlaminar shear strength of pitch-based unidirectional C–C composites. Carbon 2001;39(1):73–82.
[17] Pindera MJ, Choksi G, Hidde JS, Herakovich CT. A methodology for accurate shear characterisation of unidirectional composites. J Compos Mater 1987;21:1164–84.
[18] Ho H, Tsai MY, Morton J, Farley GL. Numerical analysis of the Iosipescu specimen for composite materials. Compos Sci Technol 1993;46(2):115–28.
[19] Bradley LR. Mechanical testing and modelling of carbon–carbon composites for aircraft disc brakes. PhD thesis, University of Bath, UK; 2003.
[20] Zhou G, Green ER, Morrison C. In-plane and interlaminar shear properties of carbon/epoxy laminates. Compos Sci Technol 1995;55(2):187–93.
[21] Gipple KL, Hoyns D. Measurement of the out-of-plane response of thick section composite materials using the V-notched beam specimen. J Compos Mater 1994;28(6):543–72.
[22] Neumeister J, Jansson S, Leckie F. The effect of fiber architecture on the mechanical properties of carbon/carbon composites. Acta Mater 1996;44(2):573–85.
[23] Hyer MW. Stress analysis of fiber-reinforced composite materials. Mechanical engineering series. McGraw-Hill International; 1998. p. 58.
[24] Kelly BT. The physics of graphite. London: Applied Science Publishers; 1981. p. 74.
[25] BS EN 658-6:1993. Advanced technical ceramics. Mechanical properties of ceramic composites at room temperature. Determination of shear strength by double punch shearing.
[26] Domnanovich A, Peterlik H, Wanner A, Kromp K. Elastic moduli and interlaminar shear strength of a bidirectional carbon/carbon composite after heat treatment. Compos Sci Technol 1995;53(1):7–12.